

Glass Armour and Shaped Charge Jets

Manfred Held

TDW-Gesellschaft für verteidigungstechnische Wirksysteme mbH, D-86523 Schrobenhausen (Germany)

Glaspanzerungen und Hohlladungsstachel

115 mm Hohlladungen wurden in 3 Kaliber Abstand gegen Glasziele zwischen 0° und 60° NATOwinkel gesprengt. Mit Doppellröntgenblitzaufnahmen wurden die Reststachelgeschwindigkeiten und die zerstörten Zonen im Stachel nach Zieldurchtritt bestimmt. Bei kleinen Winkeln sind die Spitzenbereichszonen und bei großen Winkeln die hinteren Zonen des Stachels gestört. Diese Tatsache kann damit erklärt werden, daß bei kleinen Winkeln der Kraterkollapseeffekt im Glasziel effektiv ist, was nicht mehr bei großen Winkeln der Fall ist. Bei größeren Winkeln dürften die beiden Abdeckplatten Beulblechwirkung aufweisen. Aus den Weg-Zeit-Messungen in den Restzielplatten kann zusammen mit dem Stachelfächer der Beginn der Störung des durchtretenden Stachels ermittelt werden. Hieraus kann auch die sogenannte Induktionszeit, wie schnell eine derartige Panzerung zu wirken beginnt, abgeleitet werden.

Blindages en verre et jets de charges creuses

Des charges creuses de 115 mm ont été tirées à intervalle constant de 3 calibres contre des cibles de verre inclinées entre 0° et 60° OTAN. À l'aide de doubles radiographies-éclair, on a déterminé les vitesses de jets résiduelles et les zones de jet perturbées après perforation de la cible. Il est surprenant de constater qu'aux petits angles, ce sont les zones de la pointe, et aux grands angles, les parties arrière du jet qui sont les plus perturbées. Ceci peut s'expliquer par le fait qu'aux petits angles, l'effet d'effondrement du cratère dans la cible de verre est efficace, ce qui n'est plus le cas aux grands angles. Là, les plaques de couverture du sandwich de verre sont efficaces comme blindage à effet PAC. À partir des mesures de pénétration en fonction du temps, comparées au potentiel de pénétration théorique, et avec l'éventail de jets, on peut déterminer le début de la perturbation du jet pénétrant. À partir de là, on peut également déduire un temps d'induction ou la vitesse à laquelle un tel blindage commence à interférer avec le jet.

Summary

115 mm shaped charges were fired at a constant built-in standoffs of 3 caliber against on both sides with steel plate covered glass targets from 0° to 60° NATO angles. The residual jet tip velocities and the disturbed jet regions have been analyzed from double flash X-ray pictures of the residual jet behind the target. Surprisingly under small angles the tip regions and under large angles the residual jet velocity regions have been more disturbed. This can be explained by the fact that under small angles the closure effect of glass is efficient but no more under large angles. But here the cover plates of the glass sandwich are effective as bulging armour. From the penetration time measurements, compared to the theoretical penetration potential, and together with the jet fan the jet velocities, which are no more perfectly penetrating can be defined. From this can be derived an induction time or how fast the armour will start to interfere with the passing jet.

1. Introduction

Glass has some special or so-called abnormal stopping power against shaped charge jets^(1,2). It is demonstrated that glass has a springback behaviour, respectively very fast closure effect^(1,3). The reason for this is given by the jump in the Hugoniot curve that glass is compressed to a higher density and less volume configuration under pressure which goes back immediately or at least very fast after the high pressure is relieved.

It has been known for a long time that glass has a relatively high effectiveness at zero degree incidence but reduced effectiveness under oblique angles⁽⁴⁾. Figure 1 shows the T_E effectiveness as a function of glass thickness under different angles. The T_E factor is decreasing once with increasing glass thickness but is drastically more reduced if 1" or 2" thick glass plates are oriented at oblique angles to the jet path. For this early investigation small

caliber shaped charges of nowadays poor quality—so-called Jet Guns—were used and were fired at 10" standoff.

The question now arises, what would be the stopping power of with steel plates covered glass targets under different attack angles, if larger shaped charges with much higher jet tip velocities and much higher precision of the jet are used.

2. Test Arrangement

The tests used the MILAN K with 115 mm diameter and 1.9 mm copper liner of 50° with a wave shaper. The jet tip velocity is 9.4 mm/ μ s and the mean particulation time around 200 μ s.

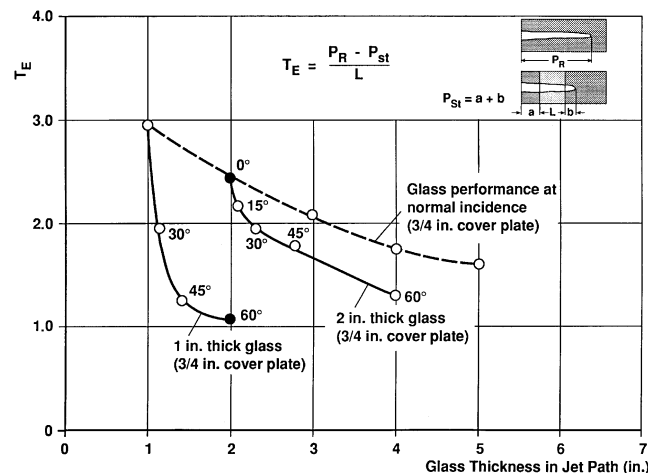


Figure 1. Jet Guns against covered glass of different thicknesses and angles (Ref. 1).

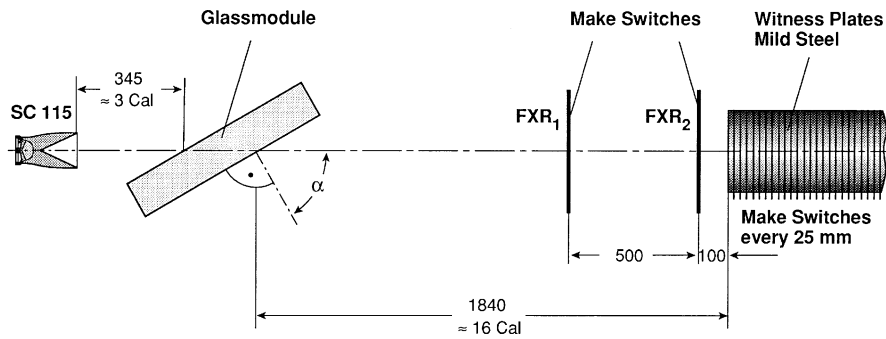


Figure 2. Test setup to see the influence of glass targets to the passing jets by flash X-ray and cratering measurements.



Figure 3. Test setup with the covered glass target under 55° .

The charge was fired against the front surface of the glass module in a constant standoff of 345 mm or 3 calibers (Figure 2). The NATO angle was changed from 0° to 60° in steps of 10° and two charges were fired additionally at 5° and 55° . The residual penetration was measured in instrumented target blocks of mild steel at 16 caliber distance behind the glass target, corresponding to 1840 mm. A first flash X-ray picture was made after 1240 mm with a make-switch and a second picture after 1740 mm from the exit side of the target. In the mild steel blocks, every 25 mm make-switches have been installed to get the penetration time history in the target places.

The warhead, supported by a styrofoam prism, followed by the glass target, arranged here at 55° , the protecting cassette for the X-ray film together with intensifier screens, the first make-switch in front of a styrofoam tube and a second make-switch in the tube and finally the instrumented target are visible in Figure 3.

3. Experimental Test Results

Figures 4 to Figure 6 show the two flash X-ray pictures of the residual jets after the glass module obtained from each test. The pictures cannot show the details which are found

on the 2 m long film strips. But the jets are differently disturbed by the glass module as a function of NATO angles.

The Table 1 gives, in addition, the shaped charge firing number, the NATO angle, the measured residual jet tip velocities v_{jRes} , the reduction in jet velocities Δv_j , the measured residual penetrations in the mild steel blocks and finally the total penetrations of the module in line of sight and the achieved residual penetrations.

The residual jet tip velocities, analysed from the double flash X-ray pictures, are decreasing with increasing NATO angles. The reduced jet portions Δv_j are therefore slightly increasing with the NATO angle where constant jet tip velocity of the MILAN with 9.4 km/s is used (Figure 7). The line of sight thickness of the glass module increases from 150 mm at 0° to 300 mm at 60° . So the larger reduction of the jet of the tip region with increasing angles can be very well understood. As expected, a nearly linear relationship exists to the path through the glass target (Figure 8).

The flash X-ray pictures show the jets are disturbed by varying amounts along their length. The regions with greater and lesser disturbance are marked in Figure 9. The jet tip region is strongly disturbed under attack at small NATO angles and undisturbed for large NATO angles, but for these larger angles the residual jets are more strongly disturbed from 5 km/s on downwards. The disturbances of the jets between the angles of 20° and 50° are not really consistent. But, with increasing angle, there is a general trend for the disturbances to more from the jet tip region to the residual jet portion. This demonstrates that this glass target has different defeating mechanisms under zero degree and large NATO angles.

At zero degree the glass acts as described in Refs. 1–3 with a so-called springback behaviour and closure effect which is effective only against the jet tip region. The following jet again perforates the “broken” glass. The residual jets are then more or less undisturbed.

Under larger attack angles to the glass modules the jet tip regions are not visibly disturbed. This means glass has nearly no effectiveness on its own if it is impacted at larger angles. But the front and rear covers of the glass plate are acting as a “bulging armour” or so-called spallation armour

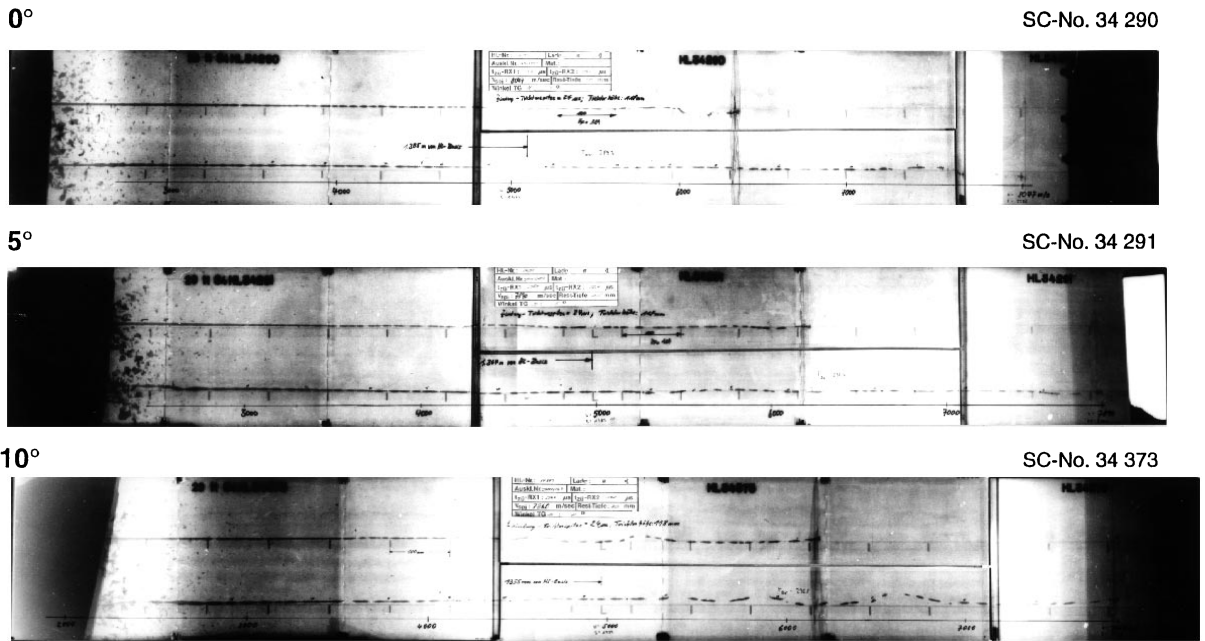


Figure 4. FXR pictures of jets behind the glass targets of 0°, 5° and 10°.

(see Ref. 1). This mechanism which needs more induction time strongly disturbs the residual jet portions.

The remarkable disturbed jet velocity regions, analysed from the FXR pictures are summarized in the Table 2.

Stronger disturbances of the jets give smaller residual penetrations in the witness blocks. This is highlighted by the tests with 10°, 40°, 55° and 60° angles where the residual penetration is under 300 mm in the witness blocks (see also Figure 9).

The measured residual penetrations P_{Res} or the total line of sight penetrations ($P_{Mod} + P_{Res}$) of Table 1 are shown as a function of NATO angle in Figure 10. Although the data have stronger scatter, the diagram shows that the residual penetration P_{Res} is decreasing with increasing NATO angle. But if the total perforation-path— $P_{Mod} + P_{Res}$ —is used then it appears that these values are more or less constant, i.e. independent of the NATO angle. This seems a surprising result.



Figure 5. FXR pictures of jets behind the glass targets of 20°, 30° and 40°.

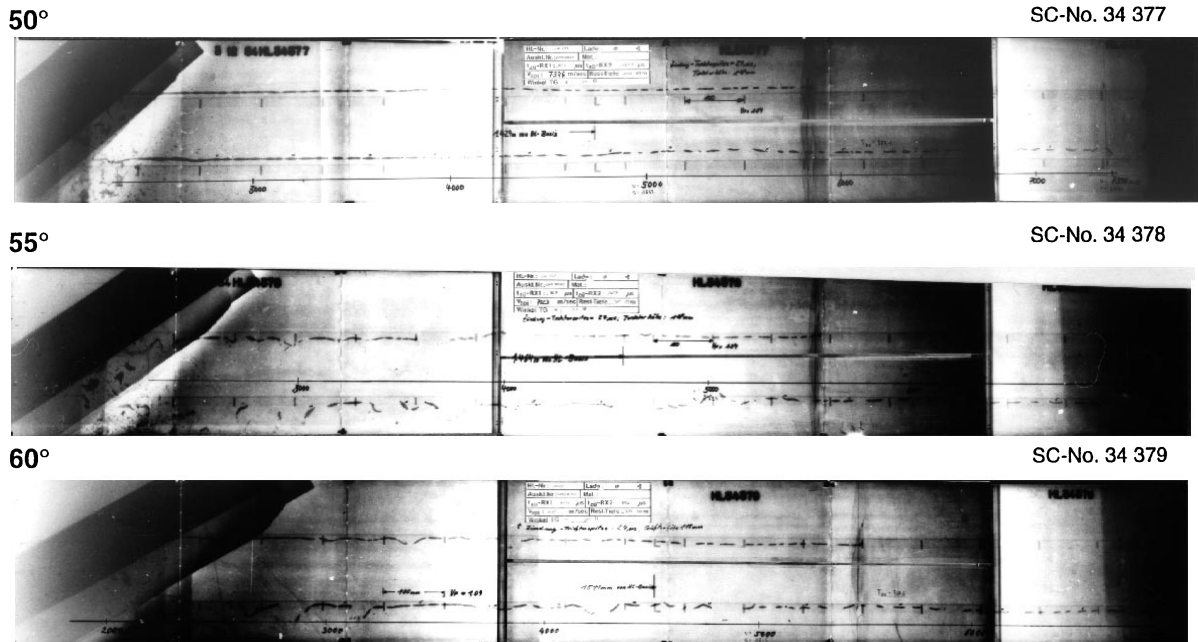


Figure 6. FXR pictures of jets behind the glass targets of 50°, 55° and 60°.

4. Cratering Measurements

In addition the penetration history in the mild steel blocks at 16 caliber standoff was measured⁽⁵⁾. As an example one time-distance measurement is shown in Figure 11. The penetration in the mild steel blocks—witness plates—follows the penetration theory⁽⁶⁾ at the beginning up to a jet velocity of around 6.7 mm/μs. This means from this velocity on, the jet deviates from the original axis and no longer arrives on the crater bottom or contributes further to penetration.

The penetration is drastically reduced as soon as the cratering diagram deviates from the theoretical prediction of penetration.

Table 1. Test Results against the Glass Target under Different Angles

SC-No	NATO angle (°)	v_{jRes} (m/s)	Δv_j (m/s)	P_{Res} (mm)	$P_{Res} + P_{Mod}$ (mm)
34290	0	8047	1353	511	664.0
34291	5	7890	1540	403	556.6
34373	10	7860	1540	303	458.4
34374	20	7872	1528	493	655.8
34376	30	7636	1764	310	486.7
34375	40	7837	(1563)	255	454.7
34377	50	7396	2104	408	646.0
34378	55	7023	2477	235	501.7
34379	60	6878	2522	268	574.0

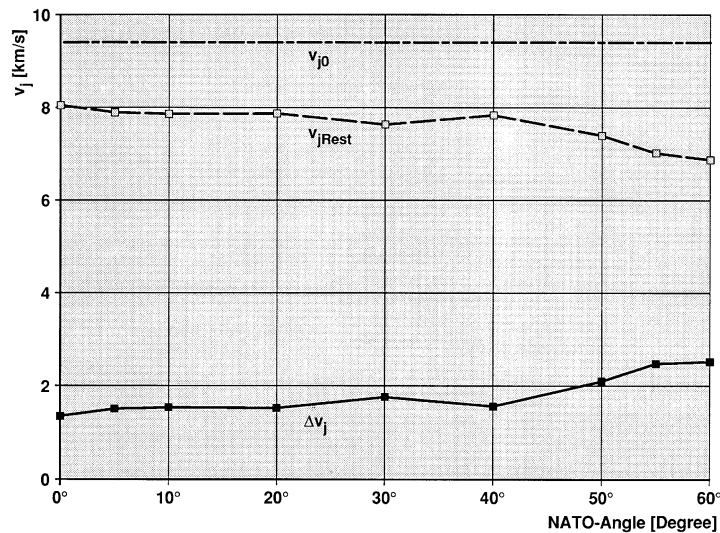


Figure 7. Residual jet tip velocities v_{jRest} and consumed jet velocities Δv_j .

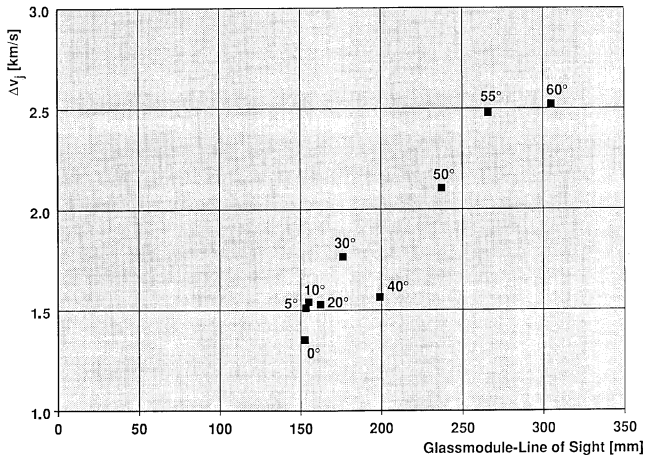


Figure 8. Consumed jet velocities as a function of perforation path in the glass targets.

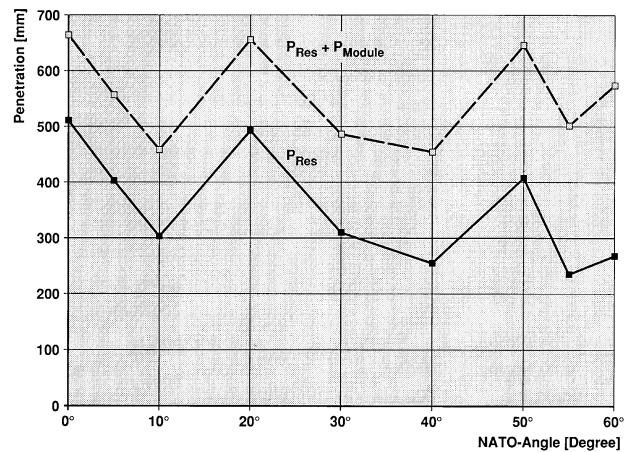


Figure 10. Residual penetrations in the mild steel blocks P_{Res} and total penetration ($P_{Res} + P_{Module}$).

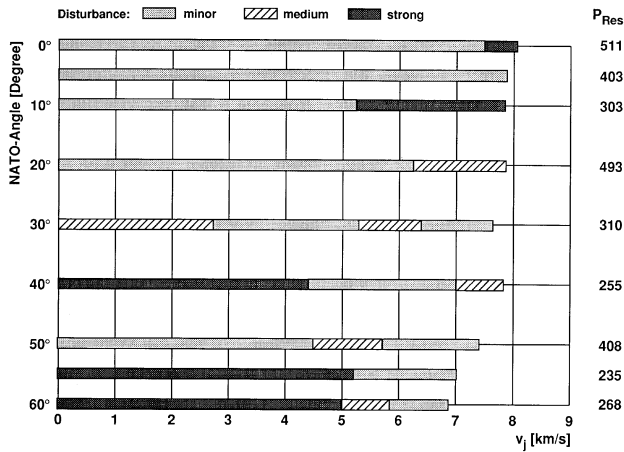


Figure 9. Disturbed jet regions and residual penetrations.

The jets are disturbed by the glass target either by the “glass effect” or the “bulging effect”. Both effects needs some time before they are working against the follow on jet velocities. For considerations the arrival times of the jet velocities on the target surface are used. This is surely a simplification. But one can select different points in the target. Under this condition—impact times on the target surface—the time differences between the arrival times of the jet tip and beginning of a disturbance on the residual penetration can be simply calculated. A virtual origin dis-

Table 2. Essential Disturbed Jet Regions

SC-No	NATO Angle (degree)	Disturbed jet regions (km/s)
34290	0	8.05–7.5
34373	10	7.9–5.3
34375	40	4.4–2.5*
34378	55	5.1–2.5*
34379	60	5.0–2.5*

* Observation limit is 2.5 km/s.

tance Z_0 of 423 mm was used. This gives an arrival time t_{j0} of the jet tip of 45 μ s. Now the time of disturbance can be simply calculated by $Z_0/v_j - Z_0/v_{j,0}$. The time differences, until disturbances are observed by the cratering measurements, are presented in Table 3, calculated with this method.

Under small angles the time interval is in the range of 10 μ s to 20 μ s before a stronger disturbance starts. These are relatively short times. With an angle of 50° the time difference is 32 μ s which demonstrates that bulging at not too large angles needs more time. With increasing angle the times are again a little decreasing as could be expected.

5. Conclusion

A covered glass target is tested under different angles with so-called precision shaped charge jets. The residual penetration decreases with increasing angle. The total penetration path in line of sight seems to be more or less constant.

It was found by the observation of the jets with flash X-ray behind the target that at small angles the tip region of the jet is disturbed and at larger angles the residual jets with velocities from about 6 mm/ μ s on. This can be explained if different defeating mechanisms are assumed. At small angle the glass with its springback behaviour or closure effect is only able to disturb the jet tip region, which does not work at large NATO angles. However, at large attack angles the front and rear plate of the glass target now works as a bulging armour. A bulging of the steel plates of this glass target, driven by the glass layer, needs some time to move.

By measuring the penetration time history, the jet velocity can be determined from where it deviates from the hydrodynamic penetration theory and then read from the jet fan lines. By using the time difference of arrival time of the jet tip, to when the jet starts to deviate from the expected

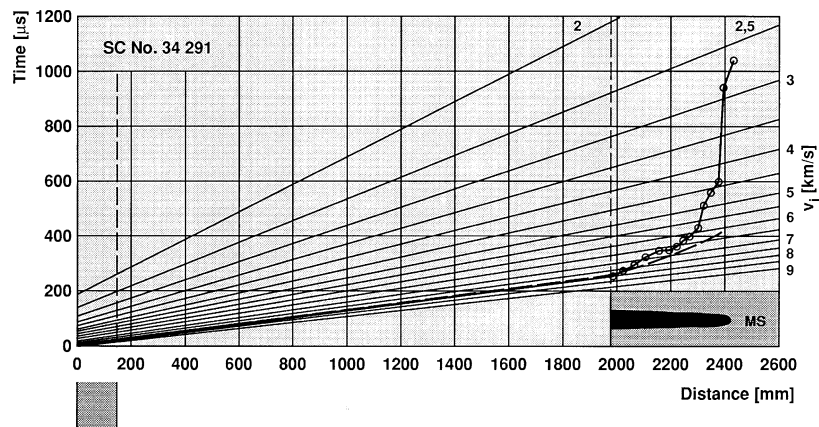


Figure 11. Example of a penetration time measurement together with the jet fan.

Table 3. Time Differences between the Arrival Times of the Jet Tip and the Beginning of a Disturbance

SC-No	NATO angle (degree)	Disturbed v_j^* (km/s)	Time to Disturbance (μ s)
34290	0	8/5.2	8/36.3
34291	5	6.7	18.1
34373	10	7.2	13.8
34374	20	7.2	13.8
34376	30	6.7	18.1
34375	40	7.1	14.6
34377	50	5.5	31.9
34378	55	6.2	23.2
34379	60	5.9	26.7

* Derived by cratering.

penetration history, the induction time of the target can be estimated.

For better understanding, the armour mechanism tests have to be made with diagnostics from the individual elements of a target arrangement. As diagnostic tools for shaped charge jet interactions with armours, flash X-ray

pictures of the residual jets and cratering measurements are especially useful.

6. References

- (1) M. Held, "Armour", *Proceedings of 14th Int. Symposium on Ballistics*, Quebec-Canada, Vol. 1 (1993).
- (2) U. Hornemann, "The Terminal Ballistic Resistance of Glass against Shaped Charge Penetration", *Proceedings of the 11th Int. Symposium on Ballistics*, Vol. II, 381–389 (1989).
- (3) G. E. Hauver, P. H. Netherwood, R. F. Benck, and A. Melani, "Penetration of Shaped Charge Jets into Glass and Crystalline Quartz", Technical Report BRL-TR-3273, 1991.
- (4) E. M. Pugh, "Defeat of Shaped Charge Weapons", Final Report, Contract No DA-36061-ORD-507, Figure 19, 1960.
- (5) M. Held, "Evaluation of Shaped Charge Penetration Efficiency by Advanced Diagnostik Techniques", *Proceedings of 6th Int. Symposium on Ballistics*, 1981, pp. 480–493.
- (6) M. Held, "Hydrodynamic Theory of Shaped Charge Jet Penetration", *Journal of Explosive and Propellants*, R.O.C.-Taiwan, 7, 9–24 (1991).

(Received November 12, 1996; Ms 69/96)